11th. World Congress on Computational Mechanics (WCCM XI)
5th. European Conference on Computational Mechanics (ECCM V)
6th. European Conference on Computational Fluid Dynamics (ECFD VI)
July 20 - 25, 2014, Barcelona, Spain

STUDY ON EFFECT OF THREE DIMENSIONAL AKIN SINGULAR ELEMENT FOR STRESS ANALYSIS OF DISSIMILAR MATERIAL JOINTS

T.Kurahashi[1], Y.Watanabe[2], T.Kondo[3] and H.Koguchi[4]

[1 4] Department of Mechanical Engineering, Nagaoka University of Technology, Kamitomioka 1603-1, Nagaokam Niigata 940-2188, JAPAN, kurahashi@mech.nagaokaut.ac.jp
[2] Electrical and Mechanical Systems Engineering Advanced Course, Advanced Course of Nagaoka National College of Technology, Nishikatakai 888, Nagaoka, Niigata 940-8532, JAPAN, ac25819x@st.nagaoka-ct.ac.jp
[3] Department of Mechanical Engineering, Nagaoka National College of Technology, Nishikatakai 888, Nagaoka, Niigata 940-8532, JAPAN, tkondo@nagaoka-ct.ac.jp

Key words: *Three-dimensional Akin Singular Element, Stress Analysis, Stress Singularity, Dissimilar Material Joints, Order of Singularity, Finite Element Eigen Analysis*

1 Introduction

In our research group, stress singular analysis is carried out based on element free Galerkin method [1], finite element method [2] and boundary element method [3]. In case that stress intensity factor around crack tip or near vertex on interface of dissimilar material joints is obtained based on methods by numerical analysis, a lot of nodes should be prepared around crack tip or near vertex on interface of dissimilar material joints. Therefore, a lot of researches investigate type of singular element. Guzina et. al. investigate difference of stress intensity factor by order of interpolation and number of nodes in 3D boundary element analysis [4]. In addition, Ong et. al. proposed several types of singular element on singular line and at vertex in potential problems based on 3D boundary element analysis [5]. In both reference, better solution is obtained by using singular element in comparison with case using conventional element.

In case of finite element analysis, Meshii et. al. and Akin have proposed singular element around crack tip[6],[7]. Moreover, Georgiou et. al. have investigated singular element in finite element flow analysis[8]. In all of papers, target model is 2D model, and it is difficult to find technical papers for application of singular element for 3D model. In this study, we focus on singular element proposed by Akin, and extend the element to 3D model, examine applicability of the element to 3D dissimilar material joint model. In addition, though order of singularity can be obtained by methodology proposed by Bogy in 2D model[9], it is difficult to analitically obtain order of singularity in 3D model. Therefore, it is necessary to numerically obtain order of singularity in case of 3D model. In this study, numerical procedure shown in references[10], [11] is applied to obtain 3D order of singularity in this study. Moreover, we clarify validity of Akin singular element extended to 3D model by mathematical formulation.

2 Shape function for conventional and Akin singular elements in FEM

In case that finite element analysis is carried out, shape function in linear tetrahedron element is written as Eq.(1).

$$\begin{cases} N_1 = 1 - \xi - \eta - \alpha \\ N_2 = \xi \\ N_3 = \eta \\ N_4 = \alpha \end{cases} \tag{1}$$

Here, N_1, N_2, N_3 and N_4 denote shape function, and ξ, η and α indicate volume coordinate. There is characteristic in shape function such that summation of shape function is equal to one. In 1976, Akin proposed special singular element considering stress distribution in singularity field under characteristic of shape function. Shape function in Akin singular element is denoted as Eq.(2).

$$\begin{cases} SN_1 = 1 - \frac{1-N_1(\xi,\eta,\alpha)}{R(\xi,\eta,\alpha)} \\ SN_2 = \frac{N_2(\xi,\eta,\alpha)}{R(\xi,\eta,\alpha)} \\ SN_3 = \frac{N_3(\xi,\eta,\alpha)}{R(\xi,\eta,\alpha)} \\ SN_4 = \frac{N_4(\xi,\eta,\alpha)}{R(\xi,\eta,\alpha)} \end{cases} \tag{2}$$

Here, Eq.(2) is defined such that origin of ξ-η coordinate system is corresponding to singularity point, and function R is written as Eq.(3). In Eq.(3), parameter λ_{vertex} indicates order of singularity at vertex.

$$R(\xi,\eta,\alpha) = (1 - N_1)^{\lambda_{vertex}} = (\xi + \eta + \alpha)^{\lambda_{vertex}} \tag{3}$$

Here, calculating derivative of shape function SN_1, SN_2, SN_3 and SN_4 with respect to x, y and z, Eq.(4) is obtained.

$$\begin{Bmatrix} \frac{\partial SN_i}{\partial x} \\ \frac{\partial SN_i}{\partial y} \\ \frac{\partial SN_i}{\partial z} \end{Bmatrix} = \begin{bmatrix} \frac{\partial x}{\partial \xi} & \frac{\partial y}{\partial \xi} & \frac{\partial z}{\partial \xi} \\ \frac{\partial x}{\partial \eta} & \frac{\partial y}{\partial \eta} & \frac{\partial z}{\partial \eta} \\ \frac{\partial x}{\partial \alpha} & \frac{\partial y}{\partial \alpha} & \frac{\partial z}{\partial \alpha} \end{bmatrix}^{-1} \begin{Bmatrix} \frac{\partial SN_i}{\partial \xi} \\ \frac{\partial SN_i}{\partial \eta} \\ \frac{\partial SN_i}{\partial \alpha} \end{Bmatrix} \tag{4}$$

Final form of right hand side vector is expressed as Eqs. Eq.(5) - Eq.(7). Eq.(4) is applied to elements including singular point and derivative of shape function for conventional linear tetrahedron element is applied to the other elements. Comparison of distribution of shape function between linear tetrahedron and Akin singular elements in case of λ_{vertex}=0.50 is shown in Fig.1.

$$\left\{ \begin{array}{c} \frac{\partial SN_1}{\partial \xi} \\ \frac{\partial SN_2}{\partial \xi} \\ \frac{\partial SN_3}{\partial \xi} \\ \frac{\partial SN_4}{\partial \xi} \end{array} \right\} = \left\{ \begin{array}{c} (1-\lambda_{vertex})\frac{\partial N_1}{\partial \xi}(1-N_1)^{-\lambda_{vertex}} \\ \frac{\partial N_2}{\partial \xi}(1-N_1)^{-\lambda_{vertex}} + \lambda_{vertex}\frac{\partial N_1}{\partial \xi}N_2(1-N_1)^{-(1+\lambda_{vertex})} \\ \frac{\partial N_3}{\partial \xi}(1-N_1)^{-\lambda_{vertex}} + \lambda_{vertex}\frac{\partial N_1}{\partial \xi}N_3(1-N_1)^{-(1+\lambda_{vertex})} \\ \frac{\partial N_4}{\partial \xi}(1-N_1)^{-\lambda_{vertex}} + \lambda_{vertex}\frac{\partial N_1}{\partial \xi}N_4(1-N_1)^{-(1+\lambda_{vertex})} \end{array} \right\} \quad (5)$$

$$\left\{ \begin{array}{c} \frac{\partial SN_1}{\partial \eta} \\ \frac{\partial SN_2}{\partial \eta} \\ \frac{\partial SN_3}{\partial \eta} \\ \frac{\partial SN_4}{\partial \eta} \end{array} \right\} = \left\{ \begin{array}{c} (1-\lambda_{vertex})\frac{\partial N_1}{\partial \eta}(1-N_1)^{-\lambda_{vertex}} \\ \frac{\partial N_2}{\partial \eta}(1-N_1)^{-\lambda_{vertex}} + \lambda_{vertex}\frac{\partial N_1}{\partial \eta}N_2(1-N_1)^{-(1+\lambda_{vertex})} \\ \frac{\partial N_3}{\partial \eta}(1-N_1)^{-\lambda_{vertex}} + \lambda_{vertex}\frac{\partial N_1}{\partial \eta}N_3(1-N_1)^{-(1+\lambda_{vertex})} \\ \frac{\partial N_4}{\partial \eta}(1-N_1)^{-\lambda_{vertex}} + \lambda_{vertex}\frac{\partial N_1}{\partial \eta}N_4(1-N_1)^{-(1+\lambda_{vertex})} \end{array} \right\} \quad (6)$$

$$\left\{ \begin{array}{c} \frac{\partial SN_1}{\partial \alpha} \\ \frac{\partial SN_2}{\partial \alpha} \\ \frac{\partial SN_3}{\partial \alpha} \\ \frac{\partial SN_4}{\partial \alpha} \end{array} \right\} = \left\{ \begin{array}{c} (1-\lambda_{vertex})\frac{\partial N_1}{\partial \alpha}(1-N_1)^{-\lambda_{vertex}} \\ \frac{\partial N_2}{\partial \alpha}(1-N_1)^{-\lambda_{vertex}} + \lambda_{vertex}\frac{\partial N_1}{\partial \alpha}N_2(1-N_1)^{-(1+\lambda_{vertex})} \\ \frac{\partial N_3}{\partial \alpha}(1-N_1)^{-\lambda_{vertex}} + \lambda_{vertex}\frac{\partial N_1}{\partial \alpha}N_3(1-N_1)^{-(1+\lambda_{vertex})} \\ \frac{\partial N_4}{\partial \alpha}(1-N_1)^{-\lambda_{vertex}} + \lambda_{vertex}\frac{\partial N_1}{\partial \alpha}N_4(1-N_1)^{-(1+\lambda_{vertex})} \end{array} \right\} \quad (7)$$

3 Mathematical Proof for Akin Singular Element Extended to 3D Model

Using shape function of Akin singular element, Unknown physical variable u is expressed as Eq.(8).

$$\begin{aligned} u(\xi,\eta,\alpha) &= SN_1u_1 + SN_2u_2 + SN_3u_3 + SN_4u_4 \\ &= 1 - \frac{1-N_1(\xi,\eta,\alpha)}{R(\xi,\eta,\alpha)}u_1 + \frac{N_2(\xi,\eta,\alpha)}{R(\xi,\eta,\alpha)}u_2 + \frac{N_3(\xi,\eta,\alpha)}{R(\xi,\eta,\alpha)}u_3 + \frac{N_4(\xi,\eta,\alpha)}{R(\xi,\eta,\alpha)}u_4 \\ &= u_1 + (u_2-u_1)\frac{\xi}{(\xi+\eta+\alpha)^{\lambda_{vertex}}} \\ &+ (u_3-u_1)\frac{\eta}{(\xi+\eta+\alpha)^{\lambda_{vertex}}} + (u_4-u_1)\frac{\alpha}{(\xi+\eta+\alpha)^{\lambda_{vertex}}} \end{aligned} \quad (8)$$

Representing ξ, η, α by spherical coordinate system, Eq.(8) is written as Eq.(9)(Fig.2).

$$\begin{aligned} u(\xi,\eta,\alpha) &= u_1 + \Big((u_2-u_1)\frac{\sin(\theta)\cos(\phi)}{s(\theta,\phi)^{\lambda_{vertex}}} \\ &+ (u_3-u_1)\frac{\sin(\theta)\sin(\phi)}{s(\theta,\phi)^{\lambda_{vertex}}} + (u_4-u_1)\frac{\cos(\theta)}{s(\theta,\phi)^{\lambda_{vertex}}}\Big)r^{1-\lambda_{vertex}} \\ &= u_1 + f_1(\theta,\phi)r^{1-\lambda_{vertex}} \end{aligned} \quad (9)$$

where $s(\theta,\phi)$ indicates $(\sin\theta\cos\phi + \sin\theta\sin\phi + \cos\theta)$.

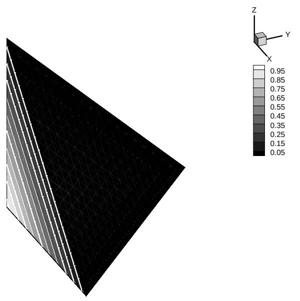

(a) N_1

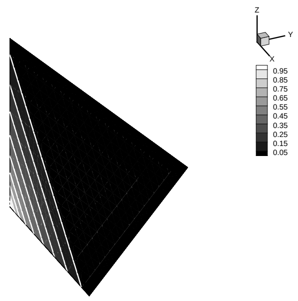

(b) SN_1 (λ_{vertex}=0.50)

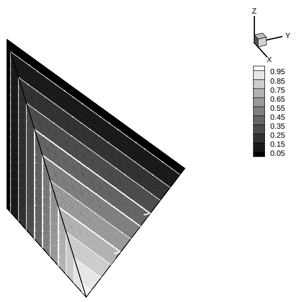

(a) N_2

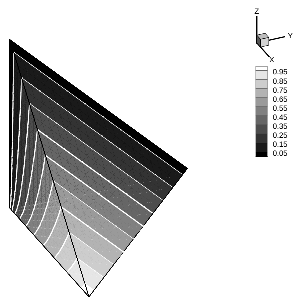

(b) SN_2 (λ_{vertex}=0.50)

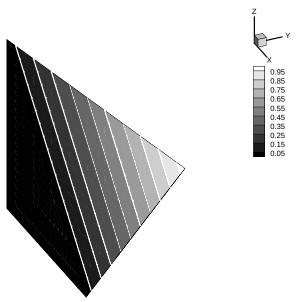

(a) N_3

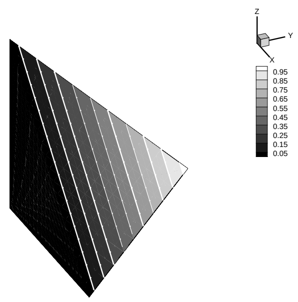

(b) SN_3 (λ_{vertex}=0.50)

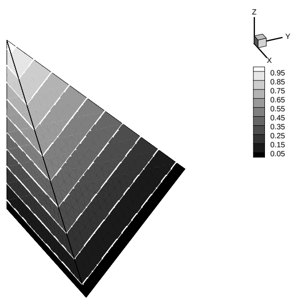

(a) N_4

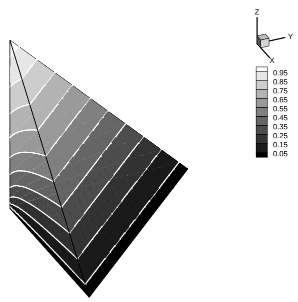

(b) SN_4 (λ_{vertex}=0.50)

Figure 1: Comparison of distribution of shape function between linear tetrahedron (N_1-N_4) and Akin singular elements (SN_1-SN_4)

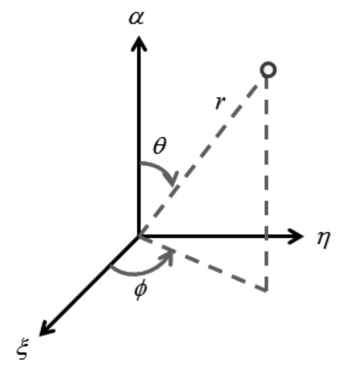

Figure 2: Spherical coordinate system

In addition, Representing coordinate x by spherical coordinate system, Eq.(10) is obtained.

$$\begin{aligned} x(\xi,\eta,\alpha) &= N_1x_1+N_2x_2+N_3x_3+N_4x_4 \\ &= x_1+(x_2-x_1)\xi+(x_3-x_1)\eta+(x_4-x_1)\alpha \\ &= x_1+\Big((x_2-x_1)\mathrm{sin}\theta\mathrm{cos}\phi+(x_3-x_1)\mathrm{sin}\theta\mathrm{sin}\phi+(x_4-x_1)\mathrm{cos}\phi\Big)r \\ &= x_1+f_2(\theta,\phi)r \end{aligned} \tag{10}$$

where $f_2(\theta,\phi)$ denotes $((x_2-x_1)\mathrm{sin}\theta\mathrm{cos}\phi+(x_3-x_1)\mathrm{sin}\theta\mathrm{sin}\phi+(x_4-x_1)\mathrm{cos}\theta)$. According to Eq.(10), Eq.(11), is obtained.

$$f_2(\theta,\phi)=\frac{1}{r}(x(\xi,\eta,\alpha)-x_1), \quad r=\frac{1}{f_2(\theta,\phi)}(x(\xi,\eta,\alpha)-x_1) \tag{11}$$

Consequently, strain ϵ_{zz} is denoted as Eq.(12).

$$\begin{aligned} \epsilon_{zz} &= \frac{\partial u(r,\theta,\phi)}{\partial z} \\ &= \frac{\partial u}{\partial r}\frac{\partial r}{\partial z}+\frac{\partial u}{\partial \theta}\frac{\partial \theta}{\partial z}+\frac{\partial u}{\partial \phi}\frac{\partial \phi}{\partial z} \\ &= (1-\lambda_{vertex})f_1(\theta,\phi)r^{-\lambda_{vertex}}\frac{1}{f_2(\theta,\phi)} \\ &+ \frac{\partial f_1(\theta,\phi)}{\partial\theta}r^{1-\lambda_{vertex}}\frac{1}{\frac{\partial f_2(\theta,\phi)}{\partial\theta}r}+\frac{\partial f_1(\theta,\phi)}{\partial\phi}r^{1-\lambda_{vertex}}\frac{1}{\frac{\partial f_2(\theta,\phi)}{\partial\phi}r} \\ &= \Big((1-\lambda_{vertex})f_1(\theta,\phi)\frac{1}{f_2(\theta,\phi)}+\frac{\partial f_1(\theta,\phi)}{\partial\theta}\frac{1}{\frac{\partial f_2(\theta,\phi)}{\partial\theta}}+\frac{\partial f_1(\theta,\phi)}{\partial\phi}\frac{1}{\frac{\partial f_2(\theta,\phi)}{\partial\phi}}\Big)r^{-\lambda_{vertex}} \\ &= C(\theta,\phi)r^{-\lambda_{vertex}} \end{aligned} \tag{12}$$

Therefore, it is found that relationship, $\epsilon_{ij},\sigma_{ij}\propto r^{-\lambda_{vertex}}$, is obtained.

4 Numerical Experiments

Analysis of stress singularity field for aluminium and mild steel bonded joint model shown in Fig.3 is carried out. Material properties are shown in Tab.1 In this study, changing element size near singularity point, relationship between minimum element size and order of singularity λ_{vertex} or intensity of stress singularity K_{1zz} is investigated. Total number of nodes and elements for each case is shown in Tab.2. In Tab.2, $\Delta hmin$ indicates characteristic minimum mesh size. $\Delta hmin$ is calcutated by $\Delta hmin = (\Delta Vmin)^{(1/3)} = ((1/6) \times \Delta xmin \Delta ymin \Delta zmin)^{(1/3)}$, ,and $\Delta Vmin$ and $\Delta x_i min (i{=}1,2,3)$ represent minimum mesh volume and minimum mesh size for each direction. In addition, order of singularity λ_{vertex} near singularity point is obtained as shown in Tab.3 based on finite element eigen analysis for order of singularity in 3D model [10], [11]. Detail of this procedure is shown in Appendix. Stress analysis is carried out for each minimum mesh size

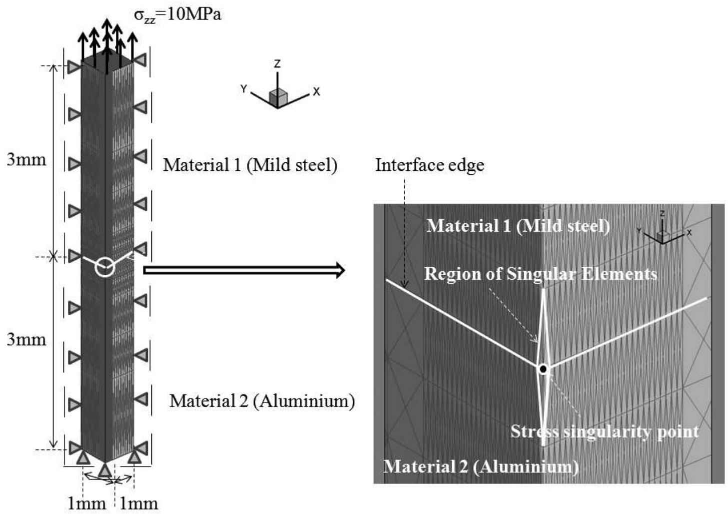

Figure 3: Finite element model and boundary condition

Table 1: Material properties

Material	Young's modulus(GPa)	Poisson's ratio
Mild steel (material 1)	216.00	0.30
Aluminium (material 2)	69.09	0.33

near singularity point shown in Tab.2, and relationship between minimum mesh size and order of singularity λ_{vertex} and intensity of stress singularity K_{1zz} is investigated based on calculation results by least square method using fitting equation $\sigma_{zz} = K_{1zz} r^{-\lambda_{vertex}}$. Distribution of σ_{zz} near singularity point for each minimum mesh size are shown in Figs.5-7, and plotted value is stress value for radius r direction from singular point O on line, θ=90deg. and ϕ=45deg. square point indicates result by using Akin singular element,

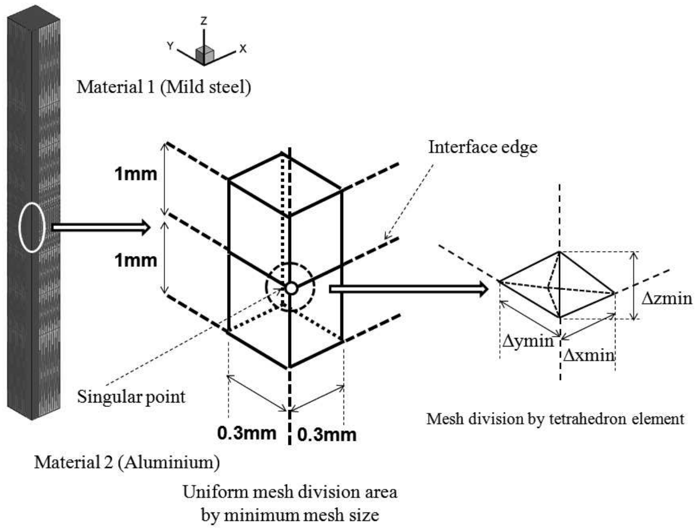

Figure 4: Set of mesh size of Akin singular element

Table 2: Number of nodes and elements for each case

Case	$\Delta xmin$=$\Delta ymin$(mm)	$\Delta zmin$(mm)	$\Delta hmin$(mm)	Nodes	Elements
1	0.0120	0.03125	0.01145	51,303	234,000
2	0.0166	0.03125	0.01430	27,881	126,144
3	0.0300	0.12500	0.03347	6,773	29,760

Table 3: Order of singularity

Characteristic root p_{vertex}	Order of singularity λ_{vertex} (λ_{vertex}=1-p_{vertex})
0.879	0.121

and circle point indicates result by normal element. In all results, it is seen that stress value near singular point obtained by Akin singular element is higher than that obtained by normal element. In addition, it is found that the result in case 1 is close to that in case 2, but small stress value is obtained even if Akin singular element is used in case of course meshes such as case 3. Moreover, lines shown in Figs.5-7 indicate fitting curve by equation $\sigma_{zz} = K_{1zz} r^{-\lambda_{vertex}}$, and relationship between each minimum mesh size and order of singularity λ_{vertex} or intensity of stress singularity K_{1zz} is shown in Fig.8 and Tab.4. From Fig.8, it is found that order of stress singularity λ_{vertex} in case of Akin singular element is close to solution obtained by finite element eigen analysis for order of singularity in 3D model, comparing to that in case of normal element. Moreover, from Tab.4, it is seen that intensity of stress singularity K_{1zz} obtained by normal element is higher than that using Akin singular element. This results denotes that if singular element is not applied to stress analysis, the intensity of stress singularity is excessively evaluated. Therefore, it can be said that the singular element should be applied to evaluate intensity of stress singularity appropriately.

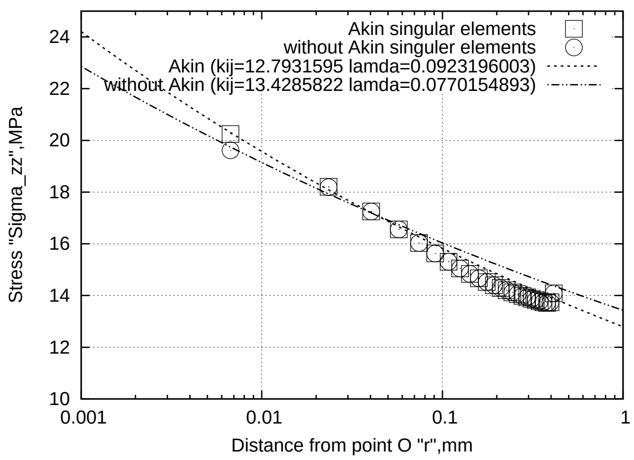

Figure 5: Comparison of distribution of stress σ_{zz} from singular point O (θ=90deg., ϕ=45deg.) in case of $\Delta hmin$=0.01145mm

Table 4: Intensity of stress singularity K_{1zz} for each case

Case	without Akin singular element	with singular element
1 ($\Delta hmin$=0.01145mm)	13.43 MPa·mm$^{0.077}$	12.79 MPa·mm$^{0.092}$
2 ($\Delta hmin$=0.01430mm)	12.41 MPa·mm$^{0.096}$	11.89 MPa·mm$^{0.111}$
3 ($\Delta hmin$=0.03347mm)	11.71 MPa·mm$^{0.045}$	11.21 MPa·mm$^{0.064}$

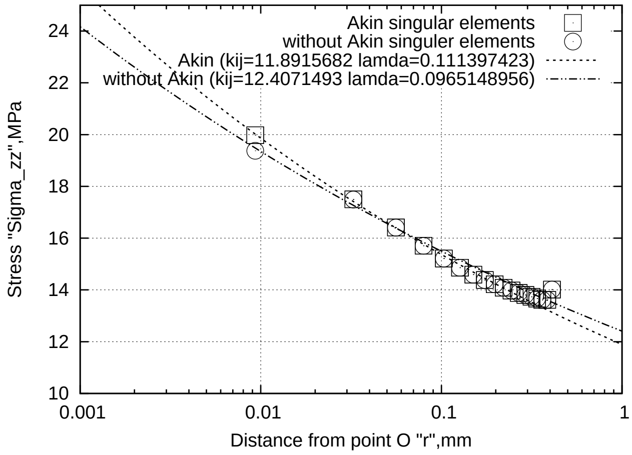

Figure 6: Comparison of distribution of stress σ_{zz} from singular point O (θ=90deg., ϕ=45deg.) in case of $\Delta hmin$=0.01430mm

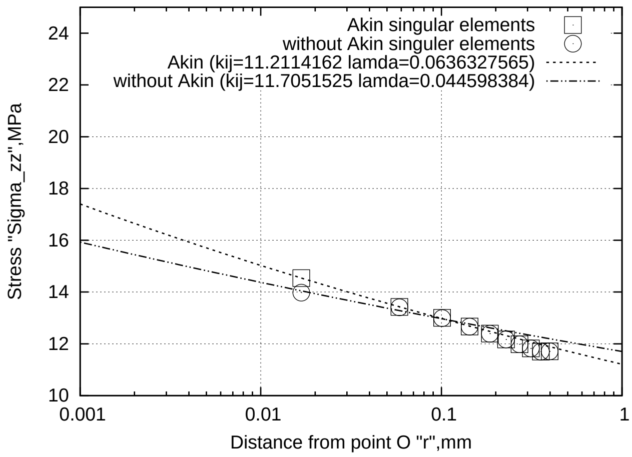

Figure 7: Comparison of distribution of stress σ_{zz} from singular point O (θ=90deg., ϕ=45deg.) in case of $\Delta hmin$=0.03347mm

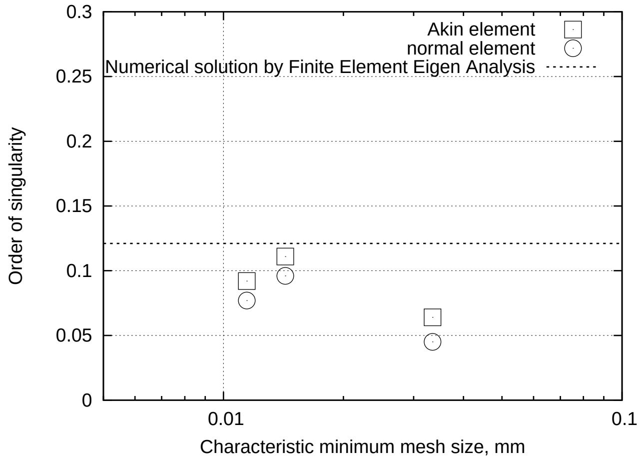

Figure 8: Relationship between minimum mesh size and order of singularity λ in case of Akin and normal elements

5 Conclusions

In this paper, a singularity element proposed by Akin was extended to 3D model using order of singularity λ_{vertex} obtained by finite element eigen analysis, and this element was applied to obtain intensity of stress singularity near vertex on interface edge of dissimilar material joints. As the computational model, aluminium-mild steel bonded structure was employed, and effect of the singular element was investigated by changing the minimum mesh size near vertex on interface. Conclusions in this study are shown as follows.

- Stress value near singular point obtained by Akin singular element is higher than that obtained by normal element.
- Order of stress singularity λ_{vertex} in case of Akin singular element is close to solution obtained by finite element eigen analysis for order of singularity in 3D model, comparing to that in case of normal element.
- If singular element is not applied to stress analysis, the intensity of stress singularity is excessively evaluated.

Acknowledgement

This work was supported by Grant-in-Aid for Young Scientists (B) (No. 25820015). We wish to thank you staff of research institute for information technology at Kyushu university for use of super computer system, FUJITSU PRIMERGY CX400.

REFERENCES

[1] T. Kurahashi, A. Ishikawa and H. Koguchi, Evaluation of Intensity of Stress Singularity for 3D Dissimilar Material Joints Based on Mesh Free Method, *11th International Conference on the Mechanical Behavior of Materials*, Procedia Engineering, Vol.10, pp.3095-3100, 2011.

[2] W. Attaporn, H. Koguchi, Intensity of Stress Singularity at a Vertex and along the Free Edges of the Interface in 3D-Dissimilar Material Joints using 3D-Enriched FEM, *Computer Modeling in Engineering & Sciences*, Vol.39, No.3, pp.237-262, 2009.

[3] H.Koguchi, J.Antonio da Costa, Analysis of the stress singularity field at a vertex in 3D-bonded structures having a slanted side surface, *International Journal of Solids and Structures*, Vol.47, Issues 22-23, pp.3131-3140, 2010.

[4] B.B.Guzina, R.Y.S.Pak, A.E.Martinez-Castro, Singular boundary elements for three-dimensional elasticity problems, *Engineering Analysis with Boundary Elements*, Vol.30, pp.623-639, 2006.

[5] E.T.Ong, K.M.Lim, Three-dimensional singular boundary elements for corner and edge singularities in potential problems, *Engineering Analysis with Boundary Elements*, Vol.29, pp.175-189, 2005.

[6] T.Meshii, K.Watanabe, Stress intensity factor error index for finite element analysis with singular elements, *Engineering Fracture Mechanics*, Vol.70, pp.657-669, 2002.

[7] J.E.Akin, The generation of elements with singularities, *International Journal for Numerical Methods in Engineering*, Vol.10, pp.1249-1259, 1976.

[8] G.C.Georgiou, L.G.Olson, W.W.Schultz and S.Sagan, A singular finite element for stokes flow: the stick-slip problem, *International Journal for Numerical Methods in Fluids*, Vol.9, pp.1353-1367, 1989.

[9] D.B.Bogy, Two Edge-Bonded Elastic Wedges of Different Materials and Wedge Angles under Surface Tractions, *J. Appl. Mech.*, 38, pp.377-386, 1971.

[10] S.S.Pageau and S.B.Bigger,JR, Finite element evaluation of free-edge singular stress fields in anisotropic materials, *Int. J. Numer. in Engng.*, Vol.38, pp.2225-2239, 1995.

[11] Y.Yamada, Y.Ezawa and I.Nishiguchi, Reconsideration on singularity or crack tip problem, *Int. J. Numer. in Engng.*, Vol.14, pp.1525-1544, 1979.